

# Theoretical Determination of Multiple Exchange Couplings and Magnetic Susceptibility Data in Inorganic Solids: The Prototypical Case of $\text{Cu}_2(\text{OH})_3\text{NO}_3$

Eliseo Ruiz,<sup>\*,†,‡</sup> Miquel Llunell,<sup>‡,§</sup> Joan Cano,<sup>†,||</sup> Pierre Rabu,<sup>⊥</sup> Marc Drillon,<sup>⊥</sup> and Carlo Massobrio<sup>⊥</sup>

*Departament de Química Inorgànica, Departament de Química Física, and Centre Especial de Recerca en Química Teòrica (CERQT), Universitat de Barcelona, Diagonal 647, 08028 Barcelona, Spain, and Institució Catalana de Recerca i Estudis Avançats (ICREA) and Institut de Physique et de Chimie des Matériaux de Strasbourg (IPCMS), 23 Rue du Loess, BP 43, F-67034 Strasbourg Cedex 2, France*

*Received: November 4, 2005*

Density functional theory based on hybrid functionals and localized atomic type basis sets is employed to calculate the exchange couplings in the layered three-dimensional compound  $\text{Cu}_2(\text{OH})_3\text{NO}_3$ . We assign accurate values to the six different in-plane exchange couplings. Interlayer exchange interactions through hydrogen bonds are also quantified. The calculated exchange coupling constants are then employed to perform quantum Monte Carlo simulations to yield magnetic susceptibility data, which compare successfully with experiments. Our approach sets the foundations of a viable methodology to extract reliable magnetic susceptibilities from density functional data.

## Introduction

Low-dimensional and nanoscale magnetic materials are typically obtained by using a bottom-up approach in which molecules are taken as constitutive units.<sup>1,2</sup> Hybrid organic–inorganic compounds have opened an alternative route to the implementation of controllable nanomagnets by combining at the nanometer-scale molecular species and inorganic layered networks.<sup>3–7</sup> Outstanding examples are the layered transition metal hydroxides  $\text{M}_2(\text{OH})_3\text{X}$  (M, divalent metal; X, exchangeable anion). These systems exhibit tunable magnetic behaviors depending on the nature of the inserted species, the character of the in-plane and interplane interactions, and the interlayer separations.<sup>5–7,9–12</sup> Due to these different contributions, a precise understanding of magnetism at the atomic scale cannot rely on approximations based on the superposition of quasi isolated magnetic entities. This calls for the application of solid-state chemistry theoretical approaches to evaluate available fingerprints of the magnetic character, such as the magnetic susceptibility. To date, the extraction of precise exchange coupling constants from experiments has proved unfeasible for multiple magnetic interactions in solids, despite the well-known accuracy in the calculation of exchange constants for isolated molecules.<sup>8</sup> Linking an elaborate pattern of exchange coupling pathways to an experimental property, with no a priori approximations on the nature of the magnetic interactions, is a longstanding challenge in theoretical magnetism.

In this paper we provide a clear insight into the physical mechanism responsible for the magnetic interactions in  $\text{Cu}_2(\text{OH})_3\text{NO}_3$ , by linking spin density topologies to the macroscopic magnetic behavior of the system. We apply a new methodologi-

cal scheme based on density functional theory (DFT) combined with quantum Monte Carlo (QMC) simulations to calculate the magnetic susceptibility  $\chi$ . Exchange coupling constants are first calculated through a state-of-the-art DFT functional and then inserted in the QMC scheme giving access to  $\chi$ .  $\text{Cu}_2(\text{OH})_3\text{NO}_3$  is one of the most studied prototypes of layered compounds prone to changes of magnetic properties in response to variations of the interlayer inserted species. Therefore, it is ideally suited to grant our result a universal character applying effectively to a wide range of magnetic materials.  $\text{Cu}_2(\text{OH})_3\text{NO}_3$  is characterized by as much as six different intralayer exchange coupling constants and by nonnegligible interlayer interactions through hydrogen bonds.<sup>7,9,13,14</sup>

## Computational Details

The calculations of exchange coupling constants presented here were performed via density functional theory using the CRYSTAL-2003 package<sup>15</sup> with the B3LYP functional.<sup>16</sup> A recent review of Corà et al. provides a detailed description of this approach and of relevant applications.<sup>17</sup> In all calculations tolerance factors of 7, 7, 7, 7, and 14 were used in the evaluation of the Coulomb and exchange integrals. The convergence criterion for the energy was set to  $10^{-7}$  au. A triple- $\zeta$  basis set with a polarization function was employed with a contraction scheme (632111/33111/311) for copper atoms, (8411/411/1) for oxygen atoms, (7311/311/1) for nitrogen atoms, and (511/1) for hydrogen atoms, previously employed in periodic calculations.<sup>18</sup> A total of 112  $k$ -points were used to perform the integration of the  $k$ -dependent magnitudes in the reciprocal space, and this number was reduced to 56  $k$ -points in the case of the supercell to calculate the interlayer interaction. The B3LYP functional provides excellent results for the calculation of the exchange coupling in a wide range of transition metal compounds.<sup>8,19</sup> Adoption of the nonprojected energy of the broken symmetry solution as the energy of the low spin state is a reliable approach within the DFT framework. This is due to the cancellation of the nondynamical correlation effects as shown recently by the

\* Corresponding author. E-mail: eliseo.ruiz@qi.ub.es. Fax: +34 93 4907725.

<sup>†</sup> Departament de Química Inorgànica, Universitat de Barcelona.

<sup>‡</sup> CERQT, Universitat de Barcelona.

<sup>§</sup> Departament de Química Física, Universitat de Barcelona.

<sup>||</sup> ICREA.

<sup>⊥</sup> IPCMS.

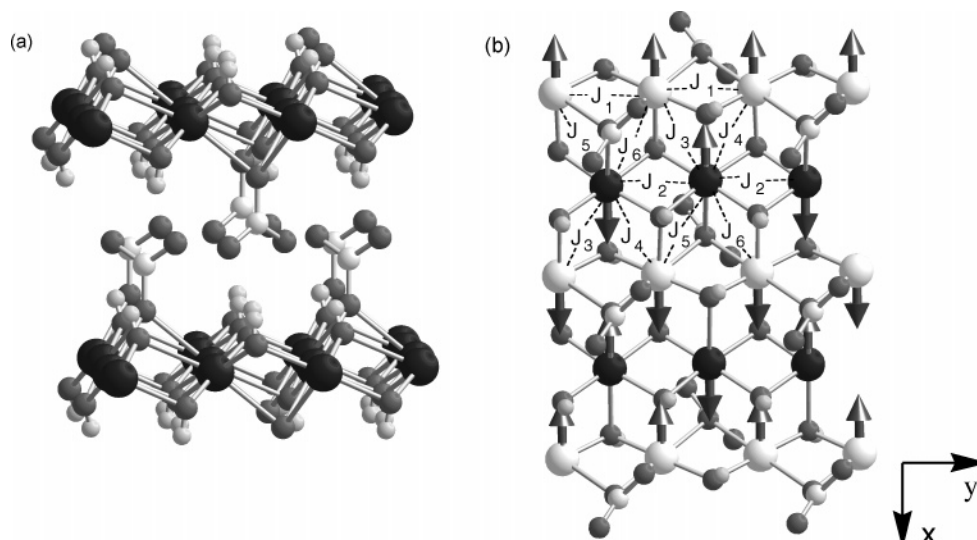


**Figure 1.** (a) Structure of the  $\text{Cu}_2(\text{OH})_3\text{NO}_3$  compound and (b) intralayer exchange pathways and spin distributions corresponding to the calculated ground state. The copper atoms are represented by large spheres, and the white ones correspond to the chains with  $\text{NO}_3$  and  $\text{OH}$  bridging ligands, while the black spheres have only  $\text{OH}$  bridging ligands. The oxygen, nitrogen and hydrogen atoms are represented by small gray spheres, from dark to bright, respectively. Exchange coupling pathways are identified with labels (from  $J_1$  to  $J_6$ ) and with dashed lines joining the corresponding pairs of Cu atoms.

Kraka and Cremer group.<sup>20,21</sup> We refer to published articles for the details of the methodology.<sup>22,23</sup> More details of its extension to periodic systems can be found in ref 24.

Exact diagonalization schemes cannot be employed directly on periodic systems to obtain magnetic susceptibilities due to the presence of an infinite number of exchange interactions. Among the different approximations to obtain the magnetic susceptibility from the calculated  $J$  values, those based on Monte Carlo simulations are widely employed. We can classify them in two groups. To the first belong those known as classical Monte Carlo based on a Metropolis algorithm, that can be applied successfully only to systems with large local spin values, for instance  $\text{Fe}^{\text{III}}$  or  $\text{Mn}^{\text{II}}$  complexes.<sup>25</sup> Members of the second are those extensions that allow treatment of quantum spin systems including local spins of  $S = 1/2$ , usually called quantum Monte Carlo methods.<sup>26</sup>

In our case the classical Monte Carlo approach cannot be employed due to the small magnetic moment of the  $\text{Cu}^{\text{II}}$  cation ( $S = 1/2$ ). We have employed the decoupled cell Monte Carlo method (DCM) proposed by Miyazawa et al.<sup>27</sup> and a modification of such an approach proposed by Homma that improves the results at low temperature (mDCM).<sup>28</sup> The basic idea is to perform the exact diagonalization only for a subsystem, the decoupled cell in this case 13  $\text{Cu}^{\text{II}}$  atoms. First, for a spin placed in the center of the subsystem, the conditional probability to be up or down is obtained from these exact diagonalization procedures. Then, it is possible to construct a Markov chain of a quantum system by using the Metropolis algorithm as in the classical Monte Carlo approach. Recently, we have successfully employed this approach for molecular systems by studying the  $\text{Fe}_8$  complex. The comparison with the results obtained with the exact diagonalization was excellent.<sup>29</sup>

## Results and Discussion

The experimental structure of the  $\text{Cu}_2(\text{OH})_3\text{NO}_3$  compound obtained by X-ray diffraction is represented in Figure 1, and it was employed in our calculations. Six different intralayer exchange coupling interactions can be distinguished, three of them corresponding to double hydroxo-bridged ligands and the others to hydroxo-nitrato ligands. The structural parameters

**TABLE 1: Exchange Coupling Constants  $J$  and Structural Parameters for the Six Intralayer Exchange Interactions of the  $\text{Cu}_2(\text{OH})_3\text{NO}_3$  Compound Calculated Using the B3LYP Functional with the Procedure Described in the Computational Details Section**

	$d(\text{Cu}\cdots\text{Cu})$ (Å)	$\text{Cu}-\text{O}-\text{Cu}$ (deg)		$J$ ( $\text{cm}^{-1}$ )
$J_1$	3.044	78.6 ( $\text{NO}_3$ )	104.1 ( $\text{OH}$ )	+28.6
$J_2$	3.045	99.3 ( $\text{OH}$ )	99.8 ( $\text{OH}$ )	-22.9
$J_3$	3.133	95.3 ( $\text{OH}$ )	104.6 ( $\text{OH}$ )	+6.9
$J_4$	3.153	95.4 ( $\text{OH}$ )	102.6 ( $\text{OH}$ )	+10.7
$J_5$	3.235	84.2 ( $\text{NO}_3$ )	110.3 ( $\text{OH}$ )	-3.54
$J_6$	3.236	85.6 ( $\text{NO}_3$ )	106.7 ( $\text{OH}$ )	+7.9

corresponding to such interactions are indicated in Table 1. Only the  $J_2$  interaction is double-bridged. In fact, for the other five coupling constants, the related exchange pathways involve at least one long  $\text{Cu}-\text{O}$  distance corresponding to the smaller  $\text{Cu}-\text{O}-\text{Cu}$  angle. Thus, these five exchange interactions can be described from the point of view of the magnetism as a single hydroxo bridging ligand.

The calculated exchange coupling constants have been obtained from the energies of seven spin arrangements of a supercell in the  $x$  direction (see Table 1). They are related to the eigenvalues of the corresponding Ising Hamiltonian and used to obtain a system of six equations with six unknowns, the  $J_a$  values.<sup>22,24</sup> The largest values for the exchange coupling correspond to the two different  $\text{Cu}^{\text{II}}$  chains,  $J_1$  being ferromagnetic and  $J_2$  antiferromagnetic (see Figure 1). This picture is different from the one proposed by Linder et al. using extended-Hückel calculations on isolated  $\text{Cu}-\text{Cu}$  dimer units. In that paper, all interactions were found to be antiferromagnetic.<sup>13</sup> The interchain couplings are relatively weaker, featuring positive and negative values. The calculation of the energy corresponding to all possible spin distributions shows that the spin arrangement indicated in Figure 1b is the most stable one. It should be noted that the pattern of the magnetic interaction for the exchange coupling  $J_6$  (Figure 1, antiparallel alignment) does not correspond to the positive sign for  $J_6$  (Table 1). This is an unambiguous indication of competition among the different magnetic interactions, resulting in a frustration effect typical of triangular-like networks.

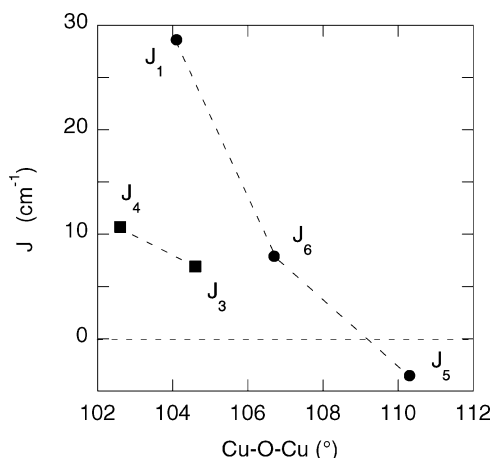


**Figure 2.** Correlation between the calculated  $J$  values corresponding to the exchange pathways with only one magnetically active bridge and the corresponding Cu–O–Cu angle of the active bridge. Black circles correspond to hydroxo–nitrate pathways, while the black squares are those with an asymmetrical double hydroxo-bridging ligand.

By focusing on correlations between the structure and the values of the exchange couplings, as observed for molecular systems,<sup>30,31</sup> we found a distinct relationship between the calculated  $J$  values and the Cu–O–Cu angle. We have considered the hydroxo bridge for the exchange pathways where only one of the bridges is magnetically active (see Figure 2). It is worth noting that, by assuming a linear correlation, the  $J_1$  value overestimates the ferromagnetic coupling when compared with the other two similar bridging ligands ( $J_5$  and  $J_6$ ). The different character of the  $J_1$  and  $J_2$  interactions is highlighted in the topology of the spin density (see Figure 3) showing essentially spin delocalization.<sup>33</sup> Thus, while the  $J_1$  interaction corresponds to a perpendicular arrangement of the magnetic orbitals, the  $J_2$  interaction arises from coplanar orbitals, due to the double bridge character, resulting in an antiferromagnetic contribution.

The exchange coupling between layers has been obtained via calculations with a supercell in the  $z$  direction. The exchange pathways between layers are through hydrogen bonds, being Cu–O–N–O···H–O–Cu, the sequence of atoms of such pathways. By assuming that all the interlayer interactions are equivalent, we obtain  $J = -7 \times 10^{-4} \text{ cm}^{-1}$ , a value essentially negligible. Despite the existence in molecule-based compounds of significant couplings through hydrogen bonds,<sup>32</sup> this result is fully consistent with the very long pathway and a very large O···H distance (around 2.2 Å) in all the interlayer interactions.

To extract the magnetic susceptibility from the calculated values, we have performed a quantum Monte Carlo (QMC) simulation<sup>24</sup> by adopting the modified decoupled cell method approach proposed by Miyazawa et al. (see Computational Details).<sup>26,27</sup> The results are shown for a single layer simulated by a  $20 \times 20$  network of paramagnetic centers, including periodic boundary conditions (see Figure 4). We point out that the maximum of susceptibility at  $T = 12 \text{ K}$  is particularly well-reproduced. Due to the difference in the height of the susceptibility maximum, the  $\chi T$  product does not follow the experimental trend, indicating that the ferromagnetic interaction  $J_1$  is likely to be overestimated within our DFT-B3LYP approach. This fact is consistent with the observation of Figure 2, where  $J_1$  is well above the linear extrapolation of the  $J_5$  and  $J_6$  values. This is confirmed by further QMC simulations performed using as starting point the  $J$  values calculated with B3LYP functional and aimed at optimizing the agreement with the experimental data (see Figure 4). Such a procedure yields the following as

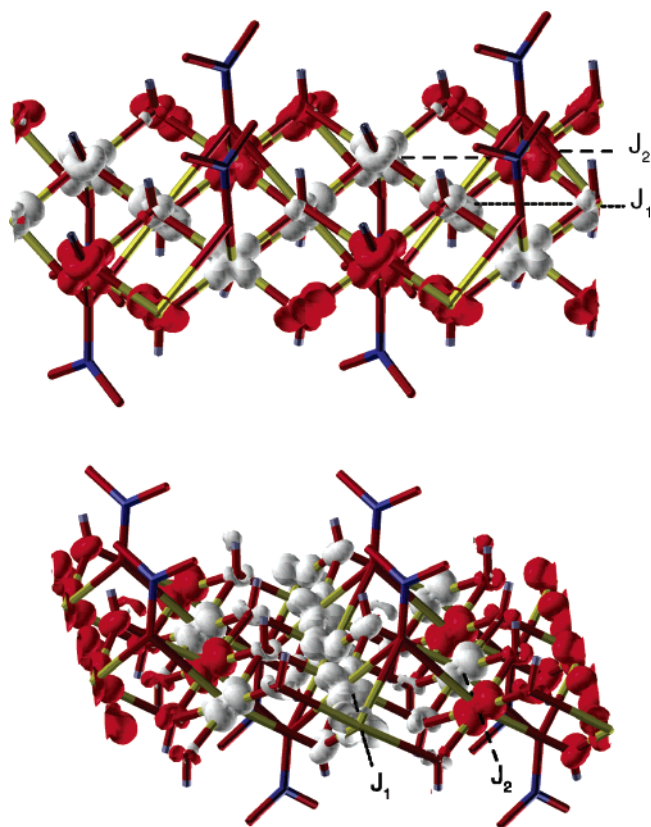


**Figure 3.** Spin density plots of a layer corresponding to the more stable spin distribution: top, along the  $x$  axis; bottom, along the  $y$  axis (see Figure 1). The chains with ferromagnetic (antiferromagnetic) coupling correspond to the  $J_1$  ( $J_2$ ) constant.

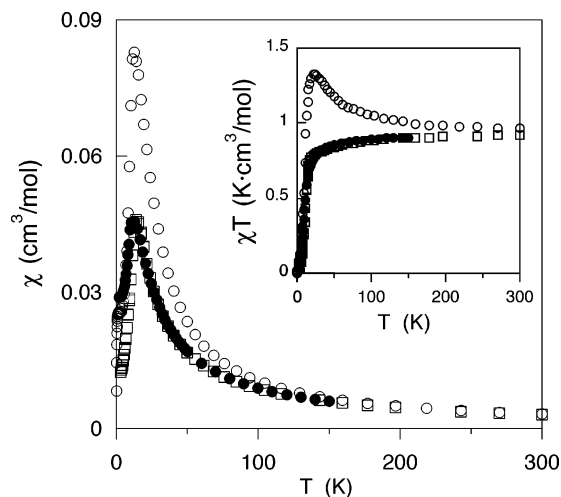


**Figure 4.** Temperature variation of the magnetic susceptibility. The black circles are the experimental data; the white circles are the results using quantum Monte Carlo simulations with the  $J$  values obtained directly from DFT calculations. The white squares correspond to the results of the fit to the experimental data ( $J_1 = +14.0 \text{ cm}^{-1}$ ,  $J_2 = -34.9 \text{ cm}^{-1}$ ,  $J_3 = +6.9 \text{ cm}^{-1}$ ,  $J_4 = +10.4 \text{ cm}^{-1}$ ,  $J_5 = -4.9 \text{ cm}^{-1}$ , and  $J_6 = +2.0 \text{ cm}^{-1}$  and  $g = 2.235$ ). Note that the optimization of the  $J$  values began from those obtained with the B3LYP functional (see Table 1 and below). Inset: Corresponding temperature variation of the  $\chi T$  product (symbols are the same as above).

final  $J$  values:  $J_1 = +14.0 \text{ cm}^{-1}$ ,  $J_2 = -34.9 \text{ cm}^{-1}$ ,  $J_3 = +6.9 \text{ cm}^{-1}$ ,  $J_4 = +10.4 \text{ cm}^{-1}$ ,  $J_5 = -4.9 \text{ cm}^{-1}$ , and  $J_6 = +2.0 \text{ cm}^{-1}$ . Note that the employed value of  $g = 2.235$  was also optimized using as starting point  $g = 2.227$  obtained from the Curie's constant of the experimental data. The main difference in comparison of the values obtained with the B3LYP functional



is the relative strength of the two strongest interactions, the antiferromagnetic  $J_2$  interaction now being the predominant one.

## Conclusion

The present study shows that the combination of electronic structure methods based on density functional theory and quantum Monte Carlo simulations yields an accurate description of the magnetic properties of extended systems with several exchange pathways. We achieved a sound theoretical determination of a measurable quantity without resorting to any approximation on the nature and the range of the magnetic interactions. This provides for the first time accurate values of magnetic interactions by considerably enriching the interpretation of the magnetic susceptibility, especially in the case of solids where the  $J$  values cannot be extracted due to the lack of mathematical expressions to fit the experimental data. Hence, we made available a manageable procedure to extract macroscopic information on magnetism through the interplay between microscopic interactions, by improving upon phenomenological schemes devised for molecule-based materials.

**Acknowledgment.** Financial support came from Dirección General de Investigación (DGI) through Project No. CTQ2005-08123-C02-02/BQU and from Comissió Interdepartamental de Ciència i Tecnologia (CIRIT) through Grant 2005SGR-00036. The computing resources at CEPBA-CIRI were generously made available through grants from the CEPBA-IBM Research Institut (CIRI).

## References and Notes

- (1) Kahn, O. *Molecular Magnetism*; VCH: New York, 1993.
- (2) *Magnetism: Molecules to Materials*; Miller, J. S., Drillon, M., Eds.; Wiley-VCH: Weinheim, Germany, 2001–2005; Vols. 1–5.
- (3) Coronado, E.; Galán-Mascarós, J.-R.; Gómez-García, C. J.; Laukhin, V. *Nature* **2000**, *408*, 447–449.
- (4) Rabu, P.; Drillon, M. *Adv. Eng. Mater.* **2003**, *5* (4), 189–210.
- (5) Rabu, P.; Drillon, M.; Awaga, K.; Fujita, W.; Sekine, T. Hybrid Organic–Inorganic Multilayer Compounds: Towards Controllable and/or Switchable Magnets. In *Magnetism: Molecules to Materials II, Molecule-Based Materials*; Miller, J. S., Drillon, M., Eds.; Wiley-VCH: Weinheim, Germany, 2001; Vol. 2, p 357.
- (6) Girtu, M.; Wynn, C. M.; Fujita, W.; Awaga, K.; Epstein, A. J. *J. Appl. Phys.* **1998**, *83*, 7378.
- (7) Maruta, G.; Nishiyama, K.; Takeda, S. *Polyhedron* **2001**, *20*, 1185.
- (8) Ruiz, E.; Alvarez, S.; Rodríguez-Fortea, A.; Alemany, P.; Pouillon, Y.; Massobrio, C. Electronic Structure and Magnetic Behavior in Polynuclear Transition-metal Compounds. In *Magnetism: Molecules to Materials II, Molecule-Based Materials*; Miller, J. S., Drillon, M., Eds.; Wiley-VCH: Weinheim, Germany, 2001; Vol. 2, p 227.
- (9) Drillon, M.; Hornick, C.; Laget, V.; Rabu, P.; Romero, F. M.; Rouba, S.; Ulrich, G.; Ziessel, R. *Mol. Cryst. Liq. Cryst.* **1995**, *273*, 125.
- (10) Drillon, M.; Panissod, P. *J. Magn. Magn. Mat.* **1998**, *188*, 93.
- (11) Fujita, W.; Awaga, K. *J. Am. Chem. Soc.* **1997**, *119*, 4563.
- (12) Drillon, M.; Panissod, P.; Rabu, P.; Souletie, J.; Ksenovontov, V.; Gülich, P. *Phys. Rev. B* **2002**, *65*, 104404.
- (13) Linder, G. G.; Atanasov, M.; Pebler, J. *J. Solid State Chem.* **1995**, *116*, 1.
- (14) Massobrio, C.; Rabu, P.; Drillon, M.; Rovira, C. *J. Phys. Chem. B* **1999**, *103*, 9387.
- (15) Saunders, V. R.; Dovesi, R.; Roetti, C.; Orlando, R.; Zicovich-Wilson, C. M.; Harrison, N. M.; Doll, K.; Civalieri, B.; Bush, I.; D'Arco, P.; Llunell, M. *CRYSTAL03*; University of Torino: Torino, Italy, 2003.
- (16) Becke, A. D. *J. Chem. Phys.* **1993**, *98*, 5648.
- (17) Corà, F.; Alfredsson, M.; Mallia, G.; Middlemiss, D. S.; Mackrodt, W. C.; Dovesi, R.; Orlando, R. *Struct. Bonding (Berlin)* **2004**, *113*, 171.
- (18) Dovesi, R.; Roetti, C.; Freyria Fava, C.; Prencipe, M.; Saunders, V. R. *Chem. Phys.* **1991**, *156*, 11.
- (19) Ruiz, E.; Cano, J.; Alvarez, S.; Alemany, P. *J. Comput. Chem.* **1999**, *20*, 1391.
- (20) Polo, V.; Graefenstein, J.; Kraka, E.; Cremer, D. *Theor. Chem. Acc.* **2003**, *109*, 22.
- (21) Polo, V.; Grafenstein, J.; Kraka, E.; Cremer, D. *Chem. Phys. Lett.* **2002**, *352*, 469.
- (22) Ruiz, E.; Rodríguez-Fortea, A.; Cano, J.; Alvarez, S.; Alemany, P. *J. Comput. Chem.* **2003**, *24*, 982.
- (23) Ruiz, E.; Cano, J.; Alvarez, S.; Polo, V. *J. Chem. Phys.* **2005**, *123*, 164110.
- (24) Ruiz, E.; Llunell, M.; Alemany, P. *J. Solid State Chem.* **2003**, *176*, 400.
- (25) Cano, J.; Journaux, Y.; Monte Carlo Simulation: A Tool To Analyze Magnetic Properties. In *Magnetism: Molecules to Materials V*; Miller, J. S., Drillon, M., Eds.; Wiley-VCH: Weinheim, Germany, 2005; Vol. 5, p 189.
- (26) *Quantum Monte Carlo Methods*; Suzuki, M., Ed.; Springer-Verlag: Berlin, 1987; Vol. 74.
- (27) Miyazawa, S.; Miyashita, S.; Makivic, M. S.; Homma, S. *Prog. Theor. Phys.* **1993**, *89*, 1167.
- (28) Homma, S. The Decoupled Cell Method of Quantum Monte Carlo Calculation. In *Quantum Monte Carlo Methods in Condensed Matter Physics*; Suzuki, M., Ed.; World Scientific: Singapore, 1993.
- (29) Ruiz, E.; Cano, J.; Alvarez, S. *Chem. Eur. J.* **2005**, *11*, 4767.
- (30) Ruiz, E.; Alemany, P.; Alvarez, S.; Cano, J. *J. Am. Chem. Soc.* **1997**, *119*, 1297.
- (31) Ruiz, E.; Alemany, P.; Alvarez, S.; Cano, J. *Inorg. Chem.* **1997**, *36*, 3683.
- (32) Desplanches, C.; Ruiz, E.; Rodríguez-Fortea, A.; Alvarez, S. *J. Am. Chem. Soc.* **2002**, *124*, 5197.
- (33) Cano, J.; Ruiz, E.; Alvarez, S.; Verdager, M. *Comments Inorg. Chem.* **1998**, *20*, 27.